

INTERACTION OF LASER RADIATION WITH MATTER. LASER PLASMA https://doi.org/10.1070/QEL16403

Localisation of intense sound produced by an optical pulsating discharge in the air

G.N. Grachev, I.B. Miroshnichenko, A.L. Smirnov,
P.A. Statsenko, V.N. Tishchenko, A.G. Berezutskii

Abstract. **It is shown that the localisation radius and the spectrum of intense sound produced by an optical pulsating discharge in the air depend on the power and repetition rate of the repetitively pulsed laser radiation, which is associated with a manifestation of the wave merging mechanism and sound absorption in the air. The experiment makes use of a CO_2 laser with a power of ~1.5 kW and a repetition rate of microsecond pulses of ~50 kHz.**

Keywords: *optical pulsating discharge, repetitively pulsed laser radiation, shock wave, spectrum, sound, localisation radius.*

An optical pulsating discharge (OPD) in gas or on the surface of solids is produced as a result of optical breakdowns by the repetitively pulsed (RP) laser radiation [1, 2]. Thermal expansion of the plasma of laser sparks is accompanied by the formation of periodic shock waves that are transformed into sound whose power constitutes 10%–20% of the RP radiation power W [3, 4]. At a high pulse repetition rate ($f \approx$ 50–100 kHz) which depends on W, there arises the wave merging mechanism (WMM) [5, 6], allowing one to control spectral characteristics of sound, which have been studied near the OPD combustion zone [3,7], i.e., at distances where the sound absorption by the air is small. An increase in the repetition rate f is accompanied by a decrease in the number of lines in the sound spectrum from tens to one at a sound frequency $\nu = f$, which corresponds to the range of ultrasonic frequencies. Periodic RP trains produce ultrasound simultaneously at a frequency $\nu = f$ and a strong low-frequency sound at a repetition rate of trains $F \ll f$. At the same time, a fraction of the sound power at low frequencies increases with increasing f. This regime is of interest for generating both infrasound and ultrasound (possibly simultaneously) when irradiating a target located at a large distance from the laser.

Previously, acoustic properties of the OPD have been studied at moderate RP radiation powers of a CO_2 laser ($W \approx$ 2 kW), when the intense sound (more than 120 dB) is localised near the OPD in the region where $r < r_{loc} \approx 1$ m. In the present work we investigate the impact of sound absorption in the air on the localisation radius r_{loc} of sound produced using the RP radiation in wide ranges of powers and pulse repetition rates. The problem is urgent for the development of promising methods based on the use of high-power RP radiation, for example, the method of controlling a supersonic flow [1, 8, 9], when the value of r_{loc} can reach tens of metres.

The experiments were conducted under the following conditions. The OPD is burning in the focusing region of the radiation beam in infinite space (in gas) or in semi-infinite space on a solid target. The duration of radiation pulses (~1 μs) is less than the time needed for the expansion of laser sparks, the energy density of radiation in the OPD zone (~5–10 J cm) is several times higher than the optical breakdown threshold in gas, which is necessary for efficient conversion of the laser pulse energy into the energy of shock waves [4]. The range of pulse repetition rates $f \approx$ 10–100 kHz corresponds to the quasi-continuous combustion of the OPP plasma and/or to the WMM manifestation. Sound attenuation is calculated using the initial spectrum [7] and the sound absorption coefficient $\alpha(\nu)$ [10].

In a laboratory experiment, the sound pressure is measured in the near zone of the discharge, where the absorption is small and the reflected sound waves have little effect on the measurements. Using the Fourier transform, the initial sound spectrum is determined. For arbitrary values of the power W and repetition rate f, the initial spectrum is determined based on the model [7].

The initial spectrum of sound produced by the OPD and its attenuation were determined using a CO_2 laser which generated the RP radiation with a power of ~1.5 kW and a pulse repetition rate of $f \approx$ 50 kHz. The peak power of the pulses (~100 kW) is insufficient for stable OPD combustion in the air, so the OPD was produced in an argon jet, where the threshold intensity of the optical breakdown is much lower than in the air. A jet with a radius of ~3 mm was emerged from the nozzle into the atmospheric air with a velocity of ~100 m s^{-1}, which ensured stable OPD combustion. The radiation was focused coaxially with the jet in the direction of the gas flow. The size of the OPD glow zone was ~5 mm. During thermal expansion, laser sparks generated the shock waves that passed into the sound waves at a distance equal to several dynamic radii $R_d = \sqrt[3]{b\delta Q/p_0} \approx 0.6$ cm, where $Q = W/f$ is the pulse energy; δQ is the energy absorbed in the laser plasma ($\delta \approx 0.5$–0.7); $b = 1$ in the case of spherical shock wave expansion (the OPD in gas) and $b = 2$ in the case of OPD on the target; and p_0 is the gas pressure.

The radial distribution of the sound pressure was measured by acoustic sensors along the line passing through the OPD spark perpendicularly to the jet axis. The initial sound spectrum was determined in the near zone: $R_1 < r < R_2$. When $r < R_1 \approx 5R_d$, the spectrum changes as a result of the interaction of shock waves with each other, while for $r > R_2 \approx \ln(W_a/W_2)/\alpha(\nu)$ – due to the sound absorption in the air.

G.N. Grachev, I.B. Miroshnichenko, A.L. Smirnov, P.A. Statsenko, V.N. Tishchenko, A.G. Berezutskii Institute of Laser Physics, Siberian Branch, Russian Academy of Sciences, prosp. Akad. Lavrent'eva 13/3, 630090 Novosibirsk, Russia; e-mail: mib_nir@ngs.ru, tvn25@ngs.ru

Received 18 April 2017
Kvantovaya Elektronika **47** (10) 911–914 (2017)
Translated by M.A. Monastyrskiy

Here W_2 is the sound power at a distance $r = R_2$; $W_a \approx \eta W$ is the sound power in the near zone; and $\eta \approx 0.1$ is the conversion efficiency of the RP radiation into sound. To estimate the upper boundary of the near field in the experiment, we assume that $W_a/W_2 \approx 1.1$, the absorption coefficients at the fundamental frequency of the spectrum $\nu = f = 50$ kHz and its overtones $\nu = 100$ and 150 kHz are 0.19, 0.55, and 0.93 m^{-1}, respectively [10]. Hereafter, the absorption coefficient is calculated at the atmospheric pressure, the humidity of 70%, and the temperature of 303 K. Hence, we obtain an estimate of ~5–20 cm for the near zone radius.

Figure 1 shows the effect of absorption in the air on the sound power spectrum. In the near zone ($r = 5$ cm), the spectrum contains the basic line at the laser pulse repetition rate $f = 50$ kHz and its overtones at multiple frequencies. At $r = 140$ cm there are no high-frequency lines in the spectrum, which is stipulated by a strong frequency dependence of the sound absorption coefficient: $\alpha(\nu) \propto \nu^2$ [10]. The spectra were obtained using the Fourier transform and normalised to the basic line amplitude in Fig. 1a. Figure 2 shows the sound intensities measured at different distances from the OPD and calculated from the formula

$$I(r) = \frac{\eta b W}{4\pi r^2}\int_0^\infty w(\nu)\exp[-2\alpha(\nu)r]\mathrm{d}\nu \qquad (1)$$

using the initial spectrum $w(\nu)$ and the sound power W for $r = 5$ cm. The solid line corresponds to a change in the intensity $I_0 = W_a/(4\pi r^2)$ in a spherical wave without allowance for absorption. It can be seen that absorption is manifested at $r > 0.2$ m.

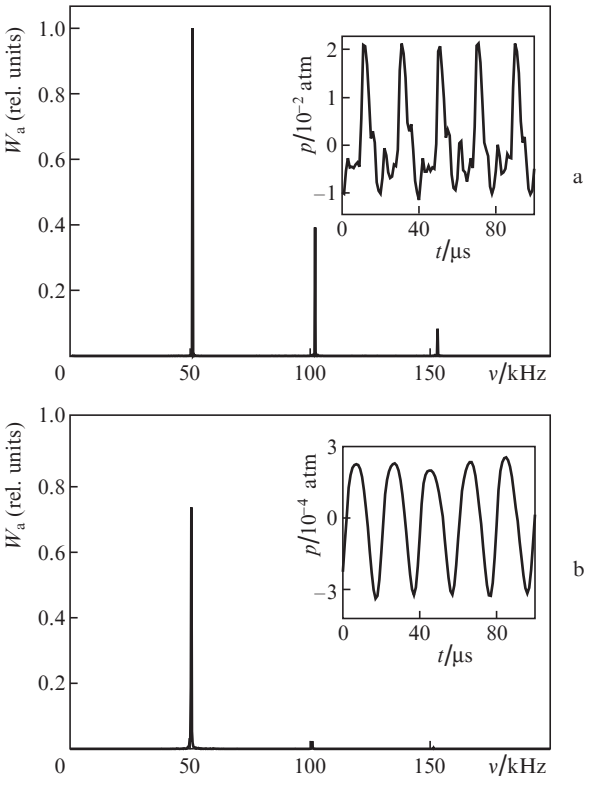

Figure 1. Sound power spectra at distances of (a) 5 and (b) 140 cm from the discharge for the OPD in the air, $f = 50$ kHz and $W \approx 1.5$ kW. The insets show the corresponding pressure oscillograms.

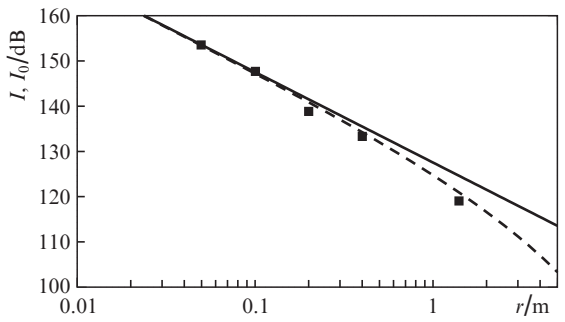

Figure 2. Sound intensity as a function of the distance to the discharge. The points are the experiment, the solid line is the calculation without taking absorption into account, the dashed curve is the calculation taking absorption into account at $b = 1$ and $\eta \approx 0.1$.

The spectrum and intensity of the sound produced by the OPD at an arbitrary power W and frequency f of the RP radiation at different distances from the OPD can be calculated using the model of work [7] describing the initial spectrum structure as a function of W and f. Figure 3 shows the boundary frequencies calculated from the formula

$$f_i = 10\left[\frac{c_0^3\omega_i^3 p_0}{b\delta W}\right]^{1/2}$$

and separating the regions of the parameters W and f, in which the initial spectrum has a qualitatively different structure. Here $i = 0, +, s$; $c_0 \approx 340$ m s^{-1} is the velocity of sound in the air; $p_0 \approx 1$ atm; the power W is taken in kilowatts; and $\omega_i = f_i R_d/c_0$ is the dimensionless RP radiation frequency that characterises the WMM effect on the shock wave structure and the sound spectrum [7]. Substituting $\omega_s \approx 0.5$, $\omega_+ \approx 1.5$, and $\omega_0 \approx 5$ in (2), we find the dependences of the boundary frequencies f_s, f_+, and f_0 on the RP radiation power. In region I, where $f < f_s$, the shock waves do not interact, the spectrum contains the main line at the RP radiation frequency f and a large number of its overtones. In region II, where $f_s < f < f_+$, the spectrum contains a line at the frequency $\nu = f$ and several overtones, the number of which decreases as the frequency f approaches f_+. In region III, where $f > f_+$, the spectrum contains a single strong line at the frequency $\nu = f$ and weak overtones. In region IV, where $f > f_0$, the spectrum contains a low-frequency line at the repetition rate of trains $F \ll f$ and its overtones. The constant pressure component of periodic sound trains is formed as a result of the WMM action, which

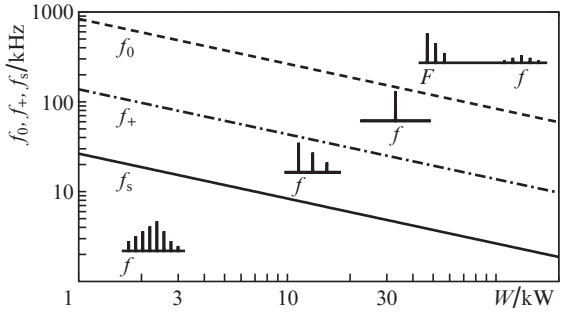

Figure 3. Boundary frequencies vs. average power of RP radiation with spherical symmetry of the sound propagation. The insets show typical sound spectra in different frequency regions.

is strongly manifested at frequencies exceeding $f_m = (f_+ + f_0)/2$, where the fraction of power at low frequencies increases with increasing f. In the range $f_m < f < f_0$, the spectrum contains a line at frequency F and overtones, and also the lines at frequencies $f \pm F$. In contrast to paper [7] in which hemispherical symmetry was considered, Fig. 3 corresponds to the spherical symmetry of sound propagation.

Figure 4 shows the sound intensities I_0, I_s, I_+, and I_m calculated at $W = 10$ kW for the boundary frequencies f_0, f_s, f_+, and f_m, respectively. In the low-frequency spectrum regions I and IV, the absorption in the localisation region of intense sound is small, and the intensity decreases due to the geometric factor: $I_0(r) = \eta b W/(4\pi r^2)$. The value of $I_s(r)$ is calculated by formula (1) for a spectrum containing the basic line and overtones, whose intensities decrease in a geometric progression with a coefficient of 0.5. For I_+ and I_m we can use the expressions that follow from (1): $I_+(r) = I_0(r)\exp[-2\alpha(f_+)r]$ and $I_m(r) = I_0(r)\exp[-2\alpha(f_m)r]$.

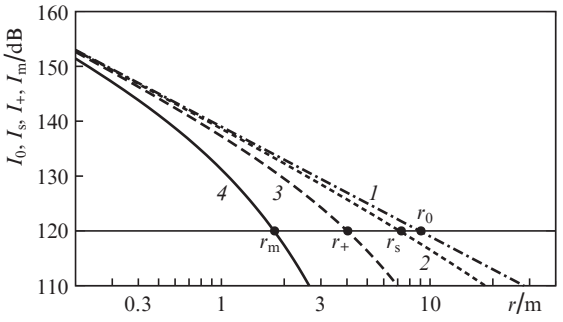

Figure 4. Dependences of the sound intensities (*1*) I_0, (*2*) I_s, (*3*) I_+, and (*4*) I_m formed by OPD in the air on r at the RP repetition rates $f = f_0, f_s, f_+$, and f_m, respectively, for $W = 10$ kW.

The sound intensity attenuation is conveniently characterised by the localisation radius r_{loc} at which I exceeds a certain level, for example, 120 dB. Figure 4 shows the radii r_0, r_s, r_+, and r_m corresponding to I_0, I_s, I_+, and I_m. At a fixed value of W, an increase in f leads to an increase in the sound absorption coefficient. However, for $f > f_m = (f_+ + f_0)/2$, as a result of the WMM action, a low-frequency component with a frequency F appears in the spectrum, a fraction of power in which increases as f approaches f_0. As a result, we obtain a nonmonotonic dependence of the sound localisation radius on the pulse repetition rate.

Figure 5 shows the dependences of the localisation radii r_0, r_s, r_+, and r_m on the power W, calculated for the boundary frequencies in accordance with the sound intensity level of 120 dB. The convergence of curves (*2*), (*3*), (*4*) and curve (*1*) with increasing W is associated with a decrease in the boundary frequencies and a corresponding decrease in the sound absorption in the air. The radius r_0 corresponds to region IV of the strong WMM action and the formation of a low-frequency sound with $\nu = F \ll f$, which is weakly absorbed at the length r_0. Here, the intensity decreases down to 120 dB as a result of the sound propagation into a full solid angle. In the low-frequency region ($f < f_s$) of RP radiation the absorption is small, and r_s differs slightly from r_0. Thus, the localisation radius of sound produced in frequency regions I and IV is proportional to $1/r^2$. In the frequency range $f_+ - f_m$, an increase in the frequency f is accompanied by a decrease in r_+ and r_m as a result of an increase in $\alpha(\nu)$.

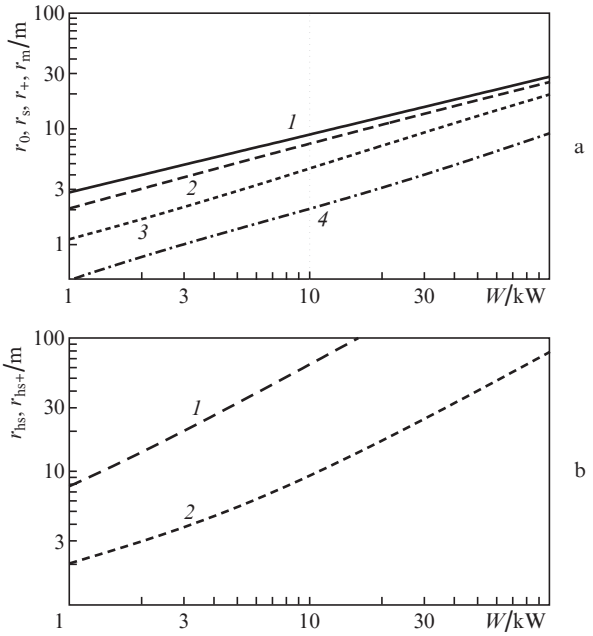

Figure 5. (a) Radii (*1*) r_0, (*2*) r_s, (*3*) r_+, and (*4*) r_m of the sound localisation at an intensity level of 120 dB for different boundary frequencies, and (b) distances (*1*) r_{hs} and (*2*) r_{hs+} at which a single line remains in the spectrum.

A change in the spectrum as a result of sound absorption by the air is possible in frequency regions I and II containing high-frequency overtones, and also in the frequency range $f_m < f < f_0$, in which the spectrum contains the lines at frequencies F and $f \pm F$. Due to a strong frequency dependence of the quantity α, high-frequency overtones are predominantly absorbed in regions I and II, while the sound at frequencies $f \pm F$ is absorbed in the range $f_m < f < f_0$. As a scale for a strong spectrum change, we can use the distance r_h at which the basic line remains in the spectrum. Figure 5b shows the dependences of the values of r_{hs} and r_{hs+} on W, calculated for the frequencies f_s and $(f_s + f_+)/2$, respectively. For definiteness, it is assumed that for $r = r_h$, the ratio of the intensity of the first overtone line (it is maximal) to the basic line intensity is 0.05. It can be seen from Fig. 5 that, in the low-frequency region ($f < f_s$), the distance at which a strong change in the spectrum occurs is larger than the localisation radius of intense sound: $r_{hs} > r_0$. For $f = (f_s + f_+)/2$ and $W < 10$ kW, the sound at the frequencies of overtones is absorbed at a distance comparable to the localisation radius r_{loc}. At large values of W, the spectrum weakly changes at distance r_{loc}, which is associated with a decrease in the boundary frequencies.

From Figs 3 and 4 we can approximately determine the spectrum structure and localisation radius of sound produced by the OPD at an arbitrary power of the RP radiation. Let $W = 10$ kW and $f = 100$ kHz. The point with such coordinates W and f is close to the boundary frequency f_m (Fig. 3), the sound with an intensity more than 120 dB is localised in the region of radius $r_m < 2$ m (Fig. 4). The point with the coordinates $W = 3$ kW and $f = 20$ kHz corresponds to region II containing a strong basic line and overtones. The localisation radius is ~3 m; the overtones are absorbed at a length of ~10 m.

Thus, the variation of the repetition rate and average power of RP radiation makes it possible to control the spectrum and localisation radius of intense ultrasound. With increasing repetition rate of laser pulses and at a fixed average

power, the localisation radius decreases due to the sound attenuation in the air. Starting from the frequency f at which the WMM appears, the localisation radius increases as a result of energy transfer from the high-frequency sound waves to the low-frequency ones. In technological RP lasers with a power up to ~10 kW, intense sound (~120 dB) is localised in a region with a radius of 2–10 m.

References

1. Tret'yakov P.K., Garanin A.F., Grachev G.N., Krainev V.L., Ponomarenko A.G., Tishchenko V.N. *Dokl. Akad. Nauk*, **351** (3), 339 (1996).
2. Grachev G.N., Ponomarenko A.G., Tishchenko V.N., Smirnov A.L., Trashkeev S.I., Statsenko P.A., Zimin M.I., Myakushina A.A., Zapryagaev V.I., Gulidov A.I., Boiko V.M., Pavlov A.A., Sobolev A.V. *Quantum Electron*., **36** (5), 470 (2006) [*Kvantovaya Elektron*., **36** (5), 470 (2006)].
3. Tishchenko V.N., Grachev G.N., Zapryagaev V.I., Smirnov A.L., Sobolev A.V. *Quantum Electron*., **32** (4), 329 (2002) [*Kvantovaya Elektron*., **32** (4), 329 (2002)].
4. Tishchenko V.N., Posukh V.G., Boyarintsev E.L., Melekhov A.V., Golobokova L.S., Miroshnichenko I.B. *Opt. Atmos. Okeana*, **25** (5), 448 (2012).
5. Tishchenko V.N., Apollonov V.V., Grachev G.N., Gulidov A.I., Zapryagaev V.I., Menshikov Ya.G., Smirnov A.L., Sobolev A.V. *Quantum Electron*., **34** (10), 941 (2004) [*Kvantovaya Elektron*., **34** (10), 941 (2004)].
6. Tishchenko V.N., Posukh V.G., Gulidov A.I., Zapryagaev V.I., Pavlov A.A., Boyarintsev E.L., Golubev M.P., Kavun I.N., Melekhov A.V., Golobokova L.S., Miroshnichenko I.B., Pavlov A.L., Shmakov A.S. *Quantum Electron*., **41** (10), 895 (2011) [*Kvantovaya Elektron*., **41** (10), 895 (2011)].
7. Grachev G.N., Dmitriev A.K., Miroshnichenko I.B., Smirnov A.L., Tishchenko V.N. *Quantum Electron*., **46** (2), 169 (2016) [*Kvantovaya Elektronika*, **46** (2), 169 (2016)].
8. Myrabo L.N., Raizer Yu.P. AIAA Paper No. 94-2551 (1994).
9. Bobarykina T.A., Malov A.N., Orishich A.M., Chirkashenko V.F., Yakovlev V.I. *Quantum Electron*., **44** (9), 836 (2014) [*Kvantovaya Elektron*., **44** (9), 836 (2014)].
10. Bass H.E., Sutherland L.C., Zuckerwar A.J., Blackstock D.T., Hester D.M. *J. Acoust. Soc. Am*., **97** (1), 680 (1995).